




The variation of structure and property of sorbitol-treated NR vulcanizates with increasing the silica loading

Abhijit Bera¹, Mohit Goswami¹, Debabrata Ganguly¹, Jyoti Prakash Rath², S. Ramakrishnan², Job Kuriakose², S. K. P. Amarnath², and Santanu Chattopadhyay^{1,*} 

¹Rubber Technology Centre, Indian Institute of Technology Kharagpur, Kharagpur 721302, West Bengal, India

²Apollo Tyres Limited, Chennai 600018, Tamil Nadu, India

Received: 23 July 2022

Accepted: 13 December 2022

Published online:

1 January 2023

© The Author(s), under exclusive licence to Springer Science+Business Media, LLC, part of Springer Nature 2022

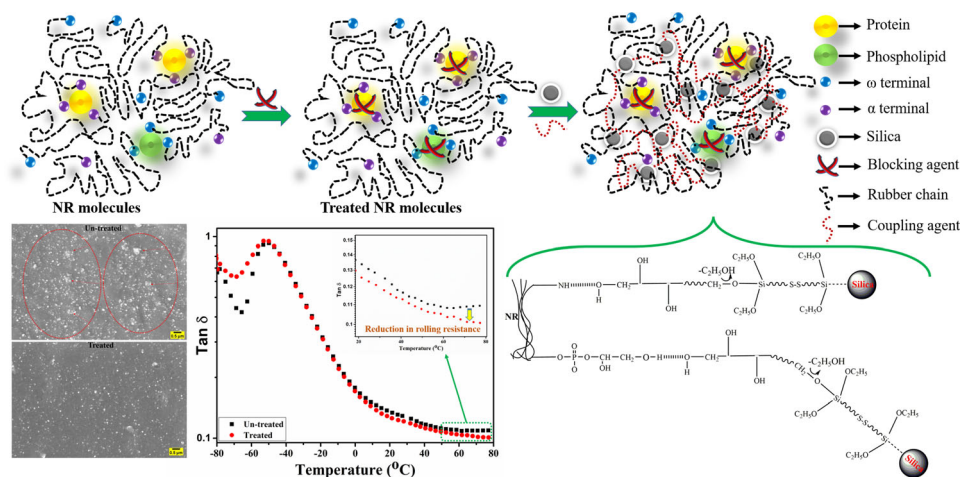
ABSTRACT

The endeavour of producing a green tyre tread compound with high silica loading is still a daunting task for all tyre industries globally. The presence of non-rubber constituents, i.e. protein and phospholipid in natural rubber (NR), disrupts the silanization reaction in the silica-filled NR composite. To get rid of that vital issue, an optimized quantity bio-based sugar alcohol “sorbitol” was introduced at the early stage of mixing as a blocking agent, for improving the silica dispersion and producing a green and sustainable tyre tread compound. A significant improvement in technical key properties like tensile strength, reinforcement index, ARI (abrasion resistance index) (~ 9%), HBU (heat build-up) (5 to 8 unit), and rolling resistance (8 to 9% reduction) was evident in sorbitol-treated NR compound, even at higher loading of silica (i.e. silica/CB: 45/5). The functional groups of NR non-rubber substance intervention interrupt the homogeneous filler dispersion, which is verified by the investigation of Payne effect and detailed morphological analysis. The constitutive modelling of the 30 phr silica-loaded sorbitol-treated and untreated NR vulcanizates was performed and fitted to find the best material model based on the correlation factor ($R^2 = 0.999$). Subsequently, by using Ogden material model constants ($N = 4$) the cross-link density of all the samples was calculated and compared with their trend of Young's modulus. Based on the overall performances, 30 phr silica-loaded sorbitol-treated compound with 20 phr carbon black was envisaged to be the best compound for tyre tread application.* As cited in Ref [38]

Handling Editor: Chris Cornelius.

Address correspondence to E-mail: santanuchat71@yahoo.com

GRAPHICAL ABSTRACT



Introduction

The rubber product manufacturing industries utilize the fillers as a cheaper or as property enhancer (reinforcing agent) [1, 2]. Usually, silica and carbon black fillers are preferred to be used as the reinforcing fillers of elastomers [2–5]. Among them, applications of silica filler are gradually increasing in rubber products, exceptionally, in tyre manufacturing industries. The incorporation of silica filler always helps to establish compatible and well-balanced tyre performance properties like heat build-up, rolling resistance, and wet grip compared to carbon black-loaded compounds [6–9]. The mechanical properties such as tear resistance, tensile strength, chip, cut, and chunking resistance can also be improved using silica filler [10–13]. The most challenging aspect is the dispersion and distribution of silica filler into a non-polar rubber matrix, especially in NR. The silica filler contains silanol groups on its surface, making it a highly polar substance. These highly polar functional groups of silica actively make bonds with each other and form agglomerated structure of fillers. The agglomerated lumps of silica particles are indeed a sign of inferior silica dispersion, which pulls down the quality of significant properties of the rubber composites [8, 14]. Although an optimal mixing of

silica-filled rubber compounds can exhibit a good dispersion of silica filler, a re-agglomeration of silica filler can happen during the time of compound storage, which is otherwise known as storage hardening [15–17]. The ultimate resolution of the earlier problems has been solved and employed since 1971. Since then, silane coupling agents or organosilanes are obtained to modify the surface of silica particles. Two different active sites of bi-functional organosilanes react with the rubber molecules and silanol groups, respectively. The formation of a strong bridge of coupling agent between rubber and filler attributes a better silica dispersion, rubber–filler interaction, and improved cure characteristics [8, 18, 19]. The excellent reinforcement of rubber compounds has been reflected through superior dynamic and mechanical properties [14, 20, 21]. The addition of a silane coupling agent protects the curatives from getting adsorbed on the surface of silica particles [22]. Currently, higher silica filler loading in solution polymerized rubber has become regular practice for PCR (passenger car radial) tyre applications. Yet, it is not commercially feasible for NR. NR primarily consists of polyisoprene, besides a minor quantity of non-rubber components, i.e. carbohydrates, proteins, and phospholipids, for about 5 to 7% w/v coexist [23]. According to a research study, it has been proved that the NR hydrocarbon is

comprised of a ω -terminal, which is connected with two trans-1,4-isoprene units, followed by the long chain of cis-1,4-isoprene (> 1000 units) and ultimately linked or ending with an α -terminal. The phospholipids are connected to the α -terminal through chemical links with the long-chain fatty acid ester groups. The protein end is linked to the ω -terminal via physical cross-links (hydrogen bond) [24–26].

The unwanted substances of NR, such as fatty acids present in phospholipid structure and proteins, have a significant contribution to upholding the superior green strength, excellent strain-induced crystallinity, and mechanical properties of the rubber [25, 27]. However, in green tyre application, incorporation of a higher quantity of silane-modified silica filler in NR is still challenging due to the interference of the functional groups of those unwanted substances. While mixing silane-modified silica filler with NR, the non-rubber constituents of NR compete with the coupling agent for the reaction with silica particles [28]. The interaction of silica and proteins originates coherently owing to hydrogen bonding between the carbonyl and amide groups of protein to the surface silanol groups of silica filler. This interruption of non-rubber components destroys the motif of reinforcement action of silica filler in the presence of a coupling agent [24]. To probe into these critical problems, bio-based sugar alcohol, “Sorbitol”, is chosen as a blocking agent for non-rubber substances rather than the complete elimination of them from the system. Unlike glucose or fructose, the functional groups of sorbitol does not go for Millard reaction with the functional groups of proteins present in NR, which basically enhances the Mooney viscosity and gel content of the natural rubber matrix [29]. However, as this particular sugar alcohol is a naturally produced inexpensive and attainable chemical, it does not have any adverse effect on natural rubber molecules. Therefore, in particular this sugar alcohol was chosen over all other 6 carbon sugar alcohols. The origin of sorbitol is glucose within the catalytic function of aldose reductase [30]. The application of sorbitol as a blocking agent in NR compound and its effectiveness has already been proved. Thereafter, most notably, the optimization study of sorbitol quantity in silica-CB-filled NR composite was distinctly exhibited [31].

In this work, we intend to enhance the silica loading eventually keeping the optimized quantity of sorbitol in raw natural rubber during mastication

unaltered. Concurrently, the untreated NR compounds were prepared with the same silica-to-carbon black ratios to visualize and quantify the difference in cure characteristics, mechanical and dynamic properties between the treated and untreated NR vulcanizates. The performance of the 30 phr silica-loaded sorbitol-treated compound was chosen as the best tyre tread compound and subsequently, taken forward for detailed temperature-dependent study by dynamic mechanical analysis and morphological estimations to predict the tyre properties and filler dispersion in NR matrix, respectively. Moreover, constitutive modelling of the 30 phr silica-loaded sorbitol-treated and untreated NR vulcanizates was performed and fitted to find the best material model based on the correlation factor (R^2) value.

Subsequently, by using Ogden material model constants the cross-link density of all the samples was calculated and compared with their trend of Young's modulus.

Materials and methods

Materials

Most of the compounding materials were used as provided by Apollo Tyres (R&D, Chennai). Those materials are: natural rubber (NR)—technically specified rubber (TSR-10)—was purchased from EQ Rubber. Carbon black (CB)-134 (SAF—super-abrasive furnace black) [$N_2SA-138.42 \text{ m}^2/\text{g}$] and highly dispersible silica (HD silica) [grade-160007/ $N_2SA-182.54 \text{ (m}^2/\text{g)}$] were supplied by Birla Carbon Black and Madhu Silica, respectively. Stearic acid, zinc oxide (ZnO), ozone protecting wax PE, antidegradant—2,2,4-trimethyl-1,2-dihydroquinoline polymer (TMQ), antiozonant and antioxidant—*N*-(1,3-dimethylbutyl)-*N*-phenyl-*p*-phenylenediamine (6PPD), curative—soluble sulphur, curing accelerator—*N*-tertiarybutyl-2-benzothiazole sulphenamide (TBBS), DPG—diphenyl guanidine and silane coupling agent—Bis-(triethoxysilylpropyl) disulphide (TESPD) were purchased from local suppliers (analytical grade). Sorbitol—bio-based sugar alcohol used as the modifying or blocking agent—was procured from Sutaria Chemicals, Mumbai.

Preparation of rubber composites

Rubber compounding formulation

The main body of formulation is depicted in Table 1 as follows:

Mixing procedure

The entire mixing process was carried out in three-stage cycles as follows:

The rotor type of the internal mixer was tangential, having the fill factor of about 0.65. After the completion of third-stage mixing in Banbury (Fig. 1), the compound was passed through a two-roll mill to attain a sheet of 8 mm thickness and stowed for 24 h at room temperature. The optimum cure time of the composites was determined by moving die rheometer (MDR 2000 Alpha Technologies, USA) at 160 °C for 30 min. According to the optimum cure time (T_c90), the moulding was operated at 160 °C using a compression moulding machine (Moore Press, United Kingdom) and cooled to ambient temperature. The images of the various mould and moulded samples are shown in supplementary section (Fig. S1).

Testing and characterization of samples

The NR composite’s rheological properties were tested at 160 °C for 30 min using an MDR (Alpha Technologies) to understand the cure characteristics (Alpha Technologies).

The hardness of all rubber vulcanizates was measured by a durometer A and IRHD combined model hardness tester (Gibitre Instrument, Italy) according

to the ASTM D 2240 test method. The results were reported as an average of four observations.

Tear (angular) and tensile (dumbbell-shaped) specimens were punched out from the moulded sheets using a hollow die punch (CEAST, Italy). The tests were performed in a universal testing machine (Zwick Roell Z010, Germany) at room temperature (25 ± 2 °C), at 500 mm/minute crosshead speed. Tear and tensile tests were carried out in line with the ASTM D 624–99 and ASTM D 412–98 methods, respectively. The abrasion samples were prepared using a three-piece, 16-cavity mould at 160 °C for 30 min. The testing was accomplished by a 6012 DIN abrasion tester (Zwick Gmbh & Co, Germany) following the testing protocol of the ISO 4649 method. Abrasion loss for each sample is expressed in terms of abrasion resistance index (ARI) according to the following equation:

$$ARI = \frac{\Delta m_r * d_t}{\Delta m_t * d_r} * 100 \tag{1}$$

where d_t is the density of test rubber vulcanizate (g/cc), m_r is reference sample mass loss (g), m_t is mass loss of the test rubber vulcanizate (g) and d_r is density of reference rubber compound (g/cc).

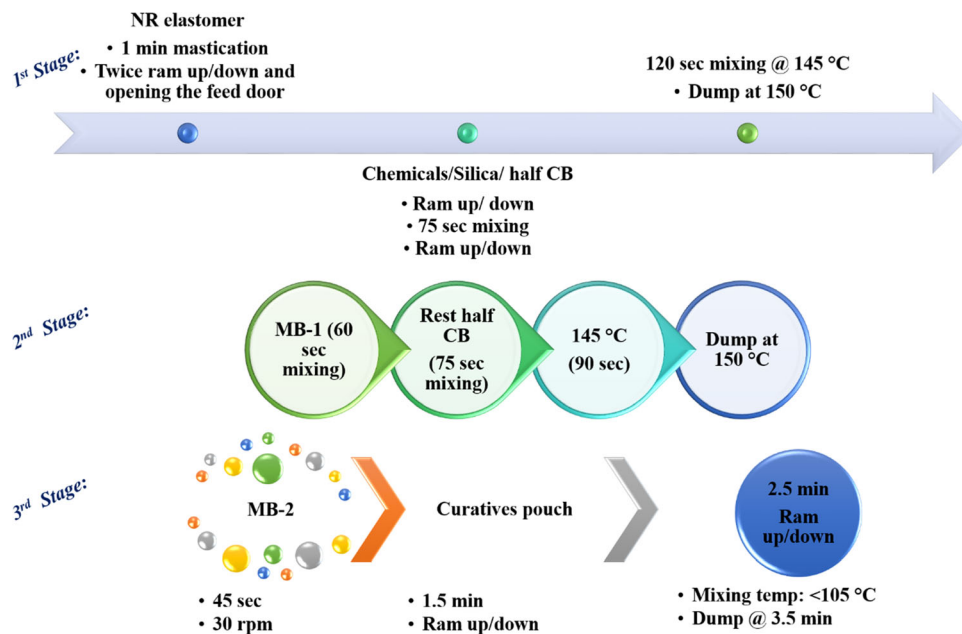
The dynamic mechanical thermal analysis was conducted using rectangle-shaped samples with dimensions of 25 mm × 10 mm × 2 mm using a dynamic mechanical analyser (DMA) (Plus1000, Metravib, France) in the tension mode. The full temperature sweep was carried out for the NR composites to realize the dynamic mechanical properties.

A simple three-piece, 16-cavity mould was utilized in making cylindrical rubber specimens having a diameter of 17.8 mm and height of 25 mm in accordance with ASTM D 623–93 for the Goodrich

Table 1 Formulation of various NR composites

Ingredients	Quantity (phr)									
	Sample designation									
	S1T	A1S1T	S2T	A1S2T	S3T	A1S3T	S4T	A1S4T	S4.5 T	A1S4.5 T
NR: TSR-10	100	100	100	100	100	100	100	100	100	100
Blocking agent (During mastication)	0	0.5	0	0.5	0	0.5	0	0.5	0	0.5
CB: N134	40	40	20	20	30	30	10	10	5	5
HD Silica	10	10	30	30	20	20	40	40	45	45

*Other chemicals—coupling agent (TESPD): 10% of silica filler, ZnO: 5, stearic acid: 2, 6PPD: 2, TMQ: 1, ozone protecting wax PE: 1, soluble sulphur: 1.5, DPG (diphenyl guanidine): 2% of silica loading, TBBS: 1.5. (phr—parts per hundred rubber)

Figure 1 Mixing flow chart.

Flexometer tester. Samples were cured at 160 °C for 30 min under pressure in the David Bridge hydraulic press. The samples were preheated for 30 min and allowed to equilibrate at 50 °C for another 25 min by getting hammered at 1800 rpm with each stroke length of 4.45 mm. The average of three samples has been reported here. The error associated with measurements in HBU was found to be ± 0.2 °C.

The rebound resilience test was performed in Schob-type rebound pendulum apparatus (Zwick Roell 5109, Germany) in accordance with the ASTM D 7121–05.

The Mullins effect of both treated and untreated vulcanizates was calculated from the hysteresis test of tensile samples (dumbbell-shaped) by UTM machine (Zwick Roell Z010, Germany) at a crosshead speed of 500 mm/minute at 25 ± 2 °C. The samples were extended to the specified strain (200%) for the first time, and after returning to the original grip position, the energy loss was measured in the first cycle from the loop area as C_1 . After that, the cyclic testing was carried out till the 12th cycle, and energy loss of the final cycle was also measured and marked as C_{12} . Subsequently, the Mullins softening was calculated using the following formula:

$$\text{Mullins softening} = \frac{C_1 - C_{12}}{C_1} * 100 \% \quad (2)$$

Scanning electron microscopy analyses were executed in a JEOL Japan JSM 7610F system under an

accelerating voltage of 15 kV. Fractography studies of the samples were carried out after cryofracture. The fractured surface was coated with a 14-Å-thick layer of Au and subsequently observed through the microscope using the secondary electron detector. Atomic force microscopy (AFM) analysis was performed using Agilent 5500 (USA) instrument. The properly cleaned moulded NR sheet samples were subjected to study the surface roughness of the vulcanizates and delineated as a phase morphology. The scanning of a $5 \times 5 \mu\text{m}$ area was carried out by a SiN_4 (silicon nitride) tip via tapping mode at a resonance frequency of 150 kHz and 42 N/m force constant, respectively.

Results and discussion

Cure characteristics

The curing characteristics of silica–CB-filled sorbitol-treated and untreated NR composites are presented in Table 2 and explained in detail with individual plot in supplementary document Fig. S2.

Mechanical properties

The hardness of various NR vulcanizates is depicted in Fig. 2. The hardness value seems maximum for 10 phr loading of silica filler. Thereafter, it is slightly decreased and displayed almost similar hardness for

the rest of the samples. Although the difference in hardness between the treated and untreated NR vulcanizates seems to be null, a clear difference in mechanical properties is demonstrated (Fig. 3) between the treated and untreated NR vulcanizates. The presence of a blocking agent in the NR compound reduced the interference of non-rubber components during silanization reaction. Hence, a continuous improvement in tensile strength and elongation at break is observed for sorbitol-treated NR compounds compared to the untreated NR compounds. The 30 phr silica-loaded NR vulcanizate exhibited a significant improvement in tensile strength and elongation at break, considered the optimum ratio of silica to CB in the presence of sorbitol. The modulus (100 and 300%) and elongation at break of NR vulcanizates displayed an opposite trend, as depicted in Fig. 3b.

The higher modulus evinced for sorbitol-treated NR vulcanizates possibly due to improved dispersion of fillers. The reinforcement index (Fig. 3c) (M300/M100) gradually raised to 20 phr loading of silica filler, and thereafter, a descending trend is noticed [32]. However, the insertion of sorbitol magically assisted in uplifting the reinforcement effect of the fillers in final NR compounds. The use of sorbitol as a blocking agent in silica–CB-filled NR compounds further showed an apparent improvement in abrasion resistance index and tear strength compared to that of the untreated compounds. A gradual decrease in tear strength is observed in the case of untreated NR vulcanizates due to the higher percentage of silica filler agglomeration [33]. After adding sorbitol in the mastication stage, the tear strength property was

Table 2 Curing data of various NR vulcanizates

Samples	Tc90 (min)	Ts2 (min)	ΔTorque (MH-ML) (dNm)
S1T	5.4	2.6	17.08
A1S1T	5.5	2.6	17.18
S2T	5.7	3.0	14.40
A1S2T	5.8	3.1	14.53
S3T	6.9	3.7	13.18
A1S3T	7.2	3.8	13.50
S4T	8.0	4.4	12.04
A1S4T	8.2	4.5	12.39
S4.5 T	8.9	5.0	11.49
A1S4.5 T	9.1	5.2	11.57

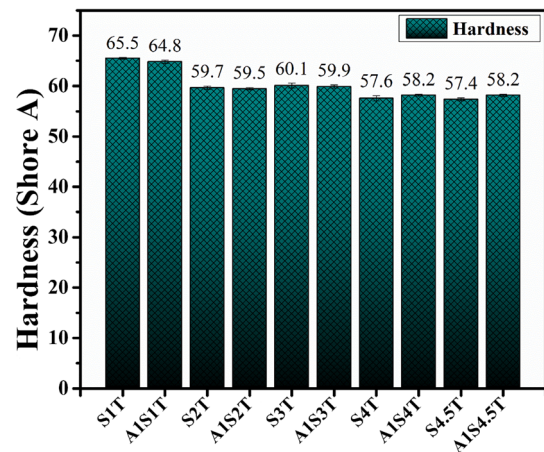


Figure 2 Hardness of NR vulcanizates.

surprisingly enhanced for 20 phr silica-loaded compounds. Then, it decreases marginally and almost steadies at a higher level as compared to that of the reference compound in the course of higher silica loading. Generally, a good filler dispersion leads to excellent abrasion resistance characteristics for the rubber vulcanizate.

Nonetheless, a stepwise decrement of ARI is viewed along with the enrichment of silica loading. Yet, a remarkable rise in ARI was witnessed in the presence of sorbitol in the NR compound. This is attributed to the superior rubber–filler interaction and filler dispersion due to less interruption of the unwanted substances present in NR, during silanization reaction [34, 35]. The rebound resilience of silica–CB-filled NR vulcanizates is illustrated in Fig. 3d. The gradual enhancement of rebound resilience is observed with the increment of silica loading due to the reduction in the CB filler in the system. The high-reinforcing filler always generates internal friction among polymer and filler besides the polymer chain displacement from the filler surface. In general, an increase in rebound resilience and decrease in compression set indicate the standard elastic property of rubber compound. Thus, according to the results of rebound resilience and dynamic compression set it is observed that 30 phr silica filler-loaded sorbitol-treated NR compound exhibited comparatively low compression set and high rebound resilience than those of untreated compounds [36, 37].

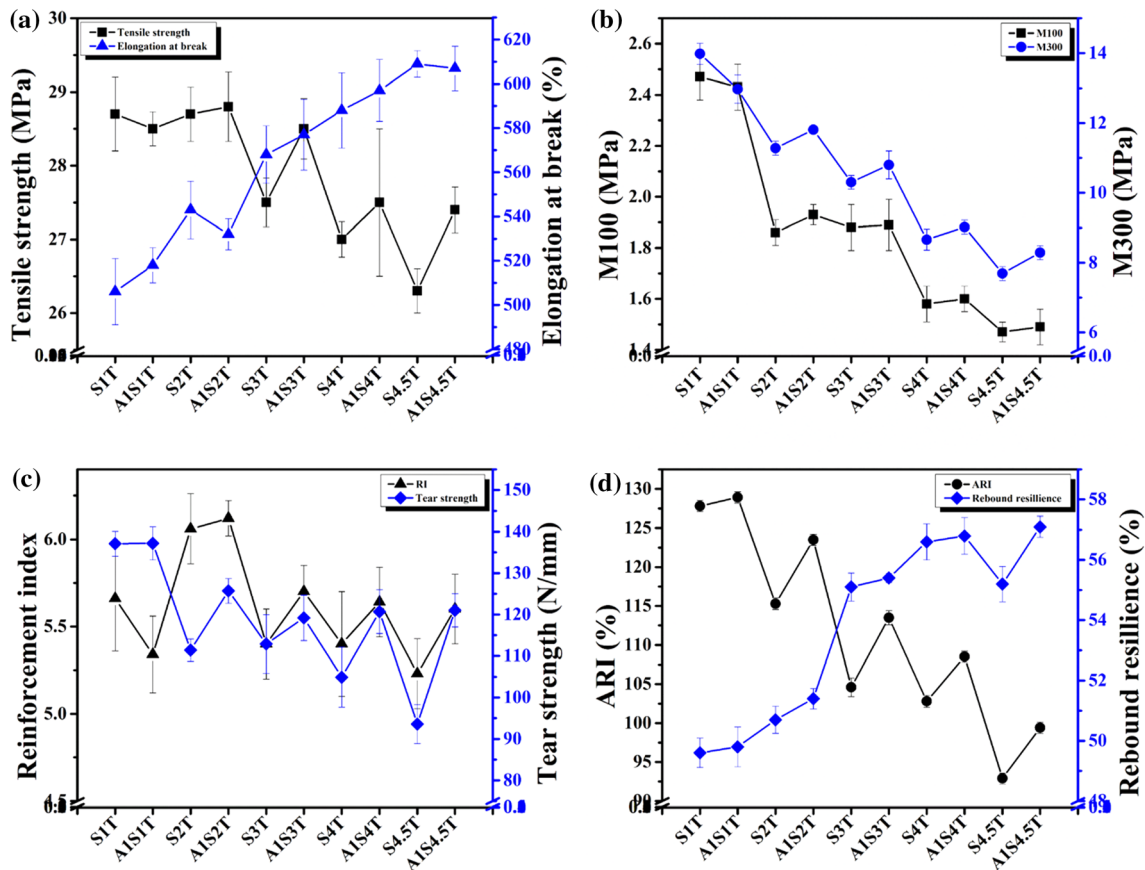


Figure 3 a Tensile strength and elongation at break, b (M100) 100 and (M300) 300% modulus, c reinforcement index and tear strength properties, d abrasion resistance index and rebound resilience of silica–CB-filled NR vulcanizates.

Dynamic properties

The dynamic compression set and heat build-up (HBU) of silica–CB-loaded composites are illustrated in Fig. 4.

The progressive increment of the compression set is noticed with the enhancement of silica loading, but the HBU displayed an opposite trend. Usually, along with the increment of silica loading, both HBU and dynamic compression set are raised due to the formation of the agglomerated structure of silica particles into the rubber composite, which attributes to inferior rubber–filler interaction and filler dispersion. In this study, the presence of the coupling agent assisted the filler dispersion, which is evident from a better rubber–filler interaction, thus leading to low filler agglomeration. In addition, the contribution of sorbitol as a blocking agent exhibited a dramatic synergistic effect of dynamic mechanical and physical properties in silane-modified silica-filled NR composites. Consequentially, during dynamic

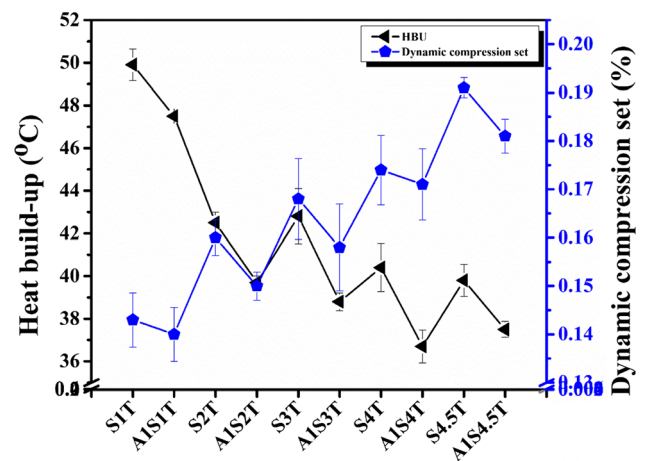


Figure 4 Heat build-up and dynamic compression set properties of NR vulcanizates.

testing, the sorbitol-treated NR vulcanizates experienced lower heat build-up than the untreated compound. Concurrently, a gradual increment in dynamic compression set value is observed in

conjunction with low to high silica loading. This is probably due to the more slippage between filler particles and rubber chains under dynamic strain. Again, the intervention of sorbitol helped to reduce the compression set property inevitably [35, 38].

After applying a cyclic tensile test at constant strain several times, the reduced required stress of the vulcanized rubber composites is called the Mullins effect or strain-softening effect [39].

The primary reasons for Mullins effect in a filled rubber compound are: (a) the slippage of molecular chains during stretching from the surface of filler particles [40]; (b) The transformation of the hard phase (high-filler-content region) to soft phase (soft filler content region) during the deformation process [41]; (c) the destruction of filler–polymer molecular interaction as well as the filler–filler aggregate structures [42]; and (d) the desorption of molecular rubber chains at the time applied external force from a rubber shell layer (i.e. adsorbed rubber molecular chains on the surface of filler) [43].

The Mullins effect percentage of the maximum CB-loaded compound is highest, which is due to smaller particle size and high surface area of carbon black (N-134). These 3D filler network structure results in filler–filler agglomeration cause the stress concentration during the cyclic stress test in uniaxial tension. The destruction of the 3D network of filler–filler agglomeration exacerbates the percentage of Mullins effect more than the destruction of polymer–filler interaction [44]. Hence, the higher CB-loaded NR vulcanizate exhibited maximum Mullins effect and gradually decreased with the enrichment of silica loading. The presence of the blocking agent

facilitated a higher number of silica–rubber chain molecules interaction. Thus, a significant reduction in the Mullins effect percentage is evidenced in Fig. 5a and b.

Based on the physical and dynamic properties, 30 phr silica filler-loaded NR composite exhibited very well performance as a whole. Therefore, this compound is taken forward for DMA study and morphological analysis to assure the tyre performance and filler dispersion, respectively, in the presence and absence of a blocking agent. The full temperature sweep study by dynamic mechanical analysis (DMA) was performed to anticipate a tyre tread compound's rolling resistance ($\tan \delta$ at 60 to 70 °C). The wet grip and ice traction can also be predicted from $\tan \delta$ values around 0 and – 20 °C, respectively. In the case of a truck and bus tyre tread application, $\tan \delta$ at 70 °C correlates well with tyre rolling resistance (RR). The lower value indicates a better rolling resistance of the tyre tread compound. Hence, according to Fig. 6a, $\tan \delta$ curve at 70 °C exhibited a lower value for the sorbitol-treated NR composites, which notify the improvement in rolling resistance property. The presence of both coupling agent and blocking agent strengthens the chemical and physical bonding between rubber molecules and filler particles. Therefore, during dynamic deformation conditions, the detachment of rubber molecules from the filler surface reduces [14].

The filler–rubber and filler–filler interactions are supreme parameters that influence the reinforcement of rubber composites. The change of storage modulus with strain confirms the filler–filler interaction level and the difference among storage modulus at high

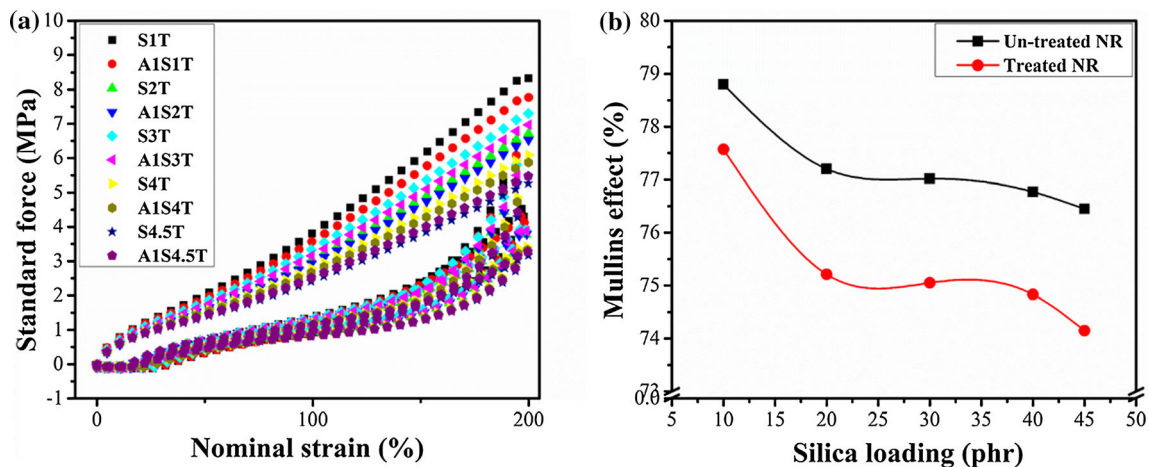


Figure 5 a Hysteresis curves and b Mullins effect of treated and untreated NR vulcanizates.

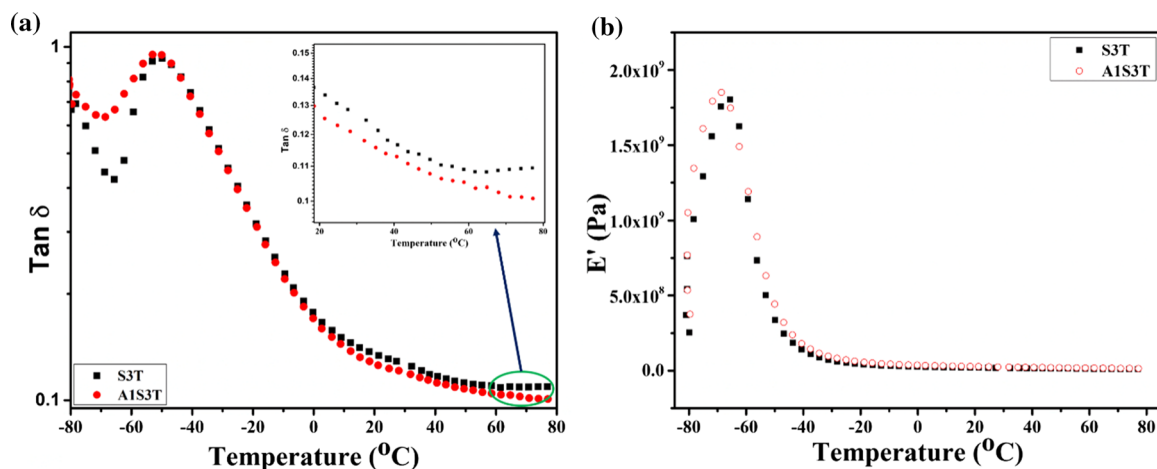


Figure 6 Full temperature sweep of DMA study. **a** $\tan \delta$ curve and its zoomed view at its higher temperature range, and **b** storage modulus of the NR vulcanizates.

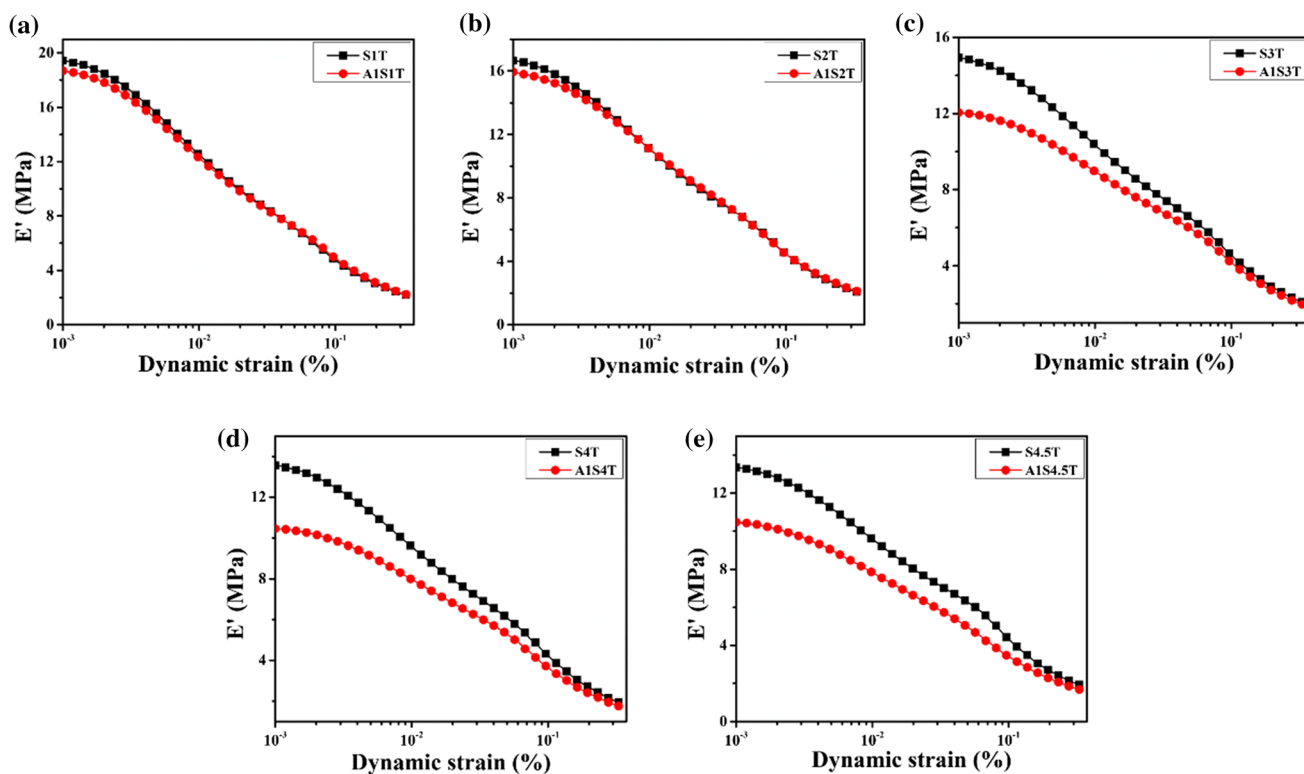


Figure 7 Strain sweep of the treated and untreated NR vulcanizates at room temperature of **a** 10/40 phr silica/CB, **b** 20/30 phr silica/CB, **c** 30/20 phr silica/CB, **d** 40/10 silica/CB, and **e** 45/5 phr silica/CB loading.

and low strains known as the Payne effect. Higher value of Payne effect ($\Delta E'$), i.e. a larger difference, indicates a higher degree of filler–filler interactions.

Figure 7 shows that the presence of a higher number of low-particle-size CB raises the Payne effect of silica–CB-filled NR compound. At maximum loading of carbon black (40 phr), the compound

distinctly exhibited higher Payne amplitude. Remarkably, a sudden reduction in the filler–filler interaction is observed from the 30 phr silica loading onwards and continued to decrease till the highest loaded silica compound with minor changes. The high surface area of carbon black N134 and smaller particle size with very confined filler particle

distances indulge the construction of the filler network and elevate the Payne effect. Moreover, in the case of high CB loading, the temperature rises faster and reduces the compound viscosity during mixing. Hence, at this low viscosity, less shearing forces are applied to disrupt the filler agglomerates, which simplify the flocculation of filler particles. On the other hand, the presence of sorbitol evidenced the reduction in the Payne effect than the untreated rubber compound indeed. That is due to its effectiveness in the silica–silane NR system, which facilitates the reduction in the filler–filler interaction between particles [14].

Morphological analysis

The field emission scanning electron microscope (FESEM) of 30 phr silica and 20 phr carbon black-loaded untreated and treated NR vulcanizates is presented in Fig. 8a and b, respectively.

The agglomeration of silica fillers is marked by the enclosed red line and clearly visible in EDX mapping for the untreated NR composite. A homogeneous dispersion of silica filler is noticed in the case of sorbitol-treated NR composite. It is worth noting that the externalization of a few phr (0.5 phr) of blocking agents at the time of mastication evolved the filler agglomeration of the NR compound to nearly zero. The exclusiveness of silane coupling agent could not attain satisfactory consequences concerning the uniform dispersion of silica filler in natural rubber elastomer. That is due to the interference of non-rubber substances of NR during silanization reaction which disrupts the interactions between rubber chain, silica particles, and silane coupling agent. Hence, the presence of sorbitol helps to block the various functional groups of non-rubber constituents by creating a bond between them. Consequently, the treated NR exhibited a clear improvement in silica dispersion, which is associated with improving the physicomechanical and dynamic properties of the tyre tread compound.

The atomic force microscopy (AFM) analysis is also performed to reconfirm the filler dispersion from vulcanizate surface topography as depicted in Fig. 9. The three-dimensional surface roughness image of the treated NR composite barely showed surface irregularities than the untreated NR composite. This attributes to the presence of more agglomerated silica particles on the surface of untreated NR vulcanizates.

The AFM images of surface roughness assured the homogeneous dispersion of silica filler in sorbitol embedded NR vulcanizate, which undoubtedly supports the results of the Payne effect as well as the SEM analysis.

TEM visualization of the silica–CB-filled untreated and treated NR vulcanizates is depicted in Fig. 10a and b, respectively. In both figures, the filler aggregates are observed as dark spots and the grey-coloured areas represent the vulcanized NR matrix network structure throughout the samples. Figure 10a displays the TEM visualization of the untreated NR vulcanizate. The higher number and broader sizes of dark regions represent broad sizes of agglomerated silica particles in the system. On the contrary, the sorbitol-treated NR vulcanizate image exhibits a homogeneous filler dispersion indicating a better filler–elastomer interaction compared to the untreated one. Thus, the interferences from TEM studies are in line with AFM and FESEM observations.

Constitutive modelling and cross-link density

The constitutive modelling of elastomeric composites has become vital for evaluating various material properties. Many material models are being proposed nowadays, but there are some limited fundamental models which are prevalent in the rubber community; a few of them are Mooney–Rivlin (Eq. 3), neo-Hookean (Eq. 4), Yeoh (Eq. 5), and Ogden (Eq. 6) [45–47].

$$W = C_{10}(I_1 - 3) + C_{01}(I_2 - 3) \tag{3}$$

$$W = C_{10}(I_1 - 3) \tag{4}$$

$$W = C_{10}(I_1 - 3) + C_{20}(I_1 - 3)^2 + C_{30}(I_1 - 3)^3 \tag{5}$$

$$W = \sum_{i=1}^N \frac{2\mu_i}{\alpha_i^2} (\lambda_1^{\alpha_i} + \lambda_2^{\alpha_i} + \lambda_3^{\alpha_i} - 3) \tag{6}$$

where W is the strain energy density function, I_1 and I_2 are strain invariants, λ is stretch ratio, and C_{10} , C_{01} , C_{20} , C_{30} , μ_i , α_i are material constants.

A relationship between stress and strain can be well established using the above equations, and the material constants can be evaluated efficiently using uniaxial test data. The materials S3T and A1S3T are fitted to find the best material model based on the correlation factor (R^2) value. Figure 11 and Table 3

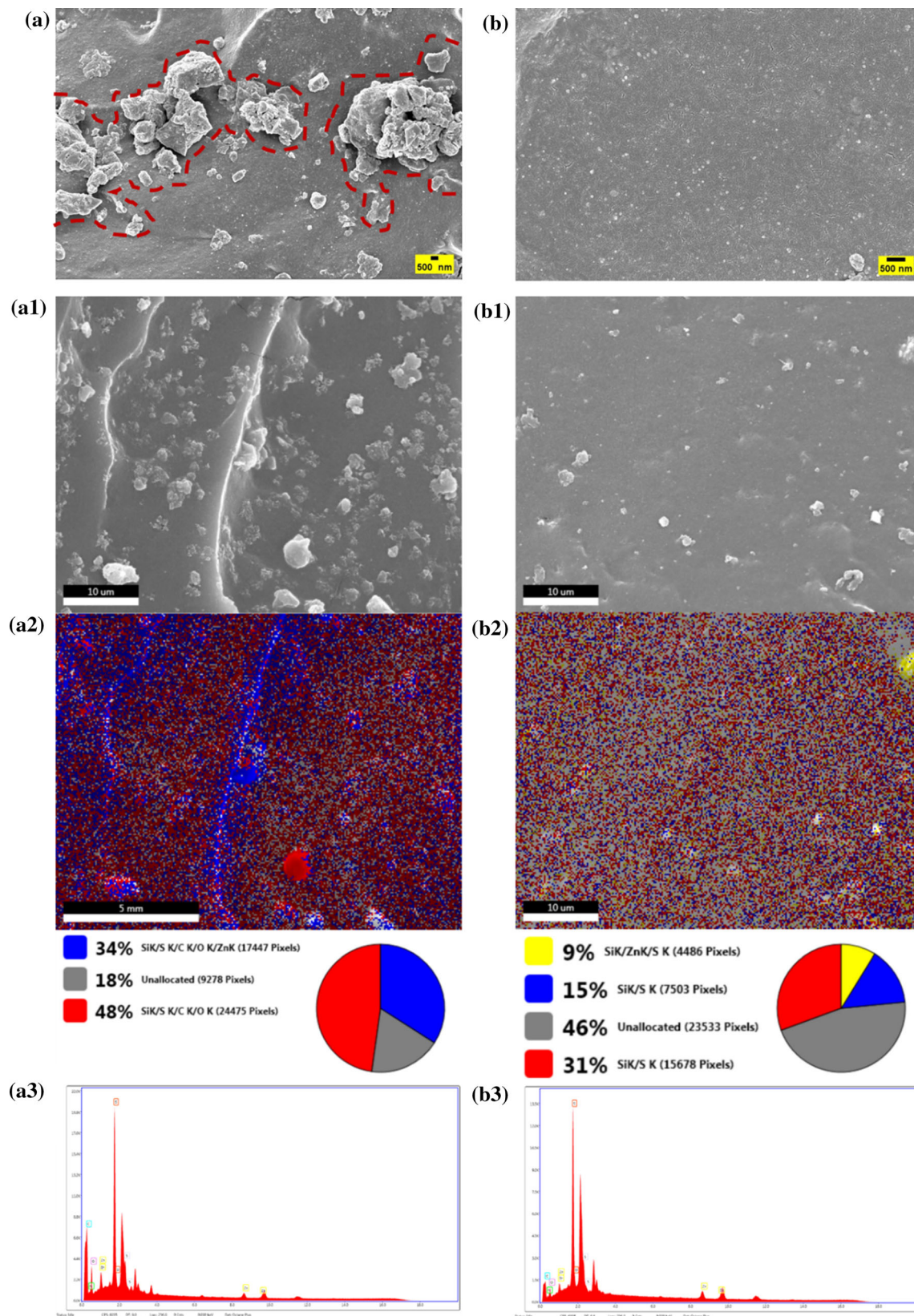


Figure 8 Field emission scanning electron microscope images of NR vulcanizates: **a** untreated NR, **b** sorbitol-treated NR composites; **a1**, **b1** and **a2**, **b2** are the images for mapping and EDX mapping of the respective samples, and **a3**, **b3** are their sum spectrum.

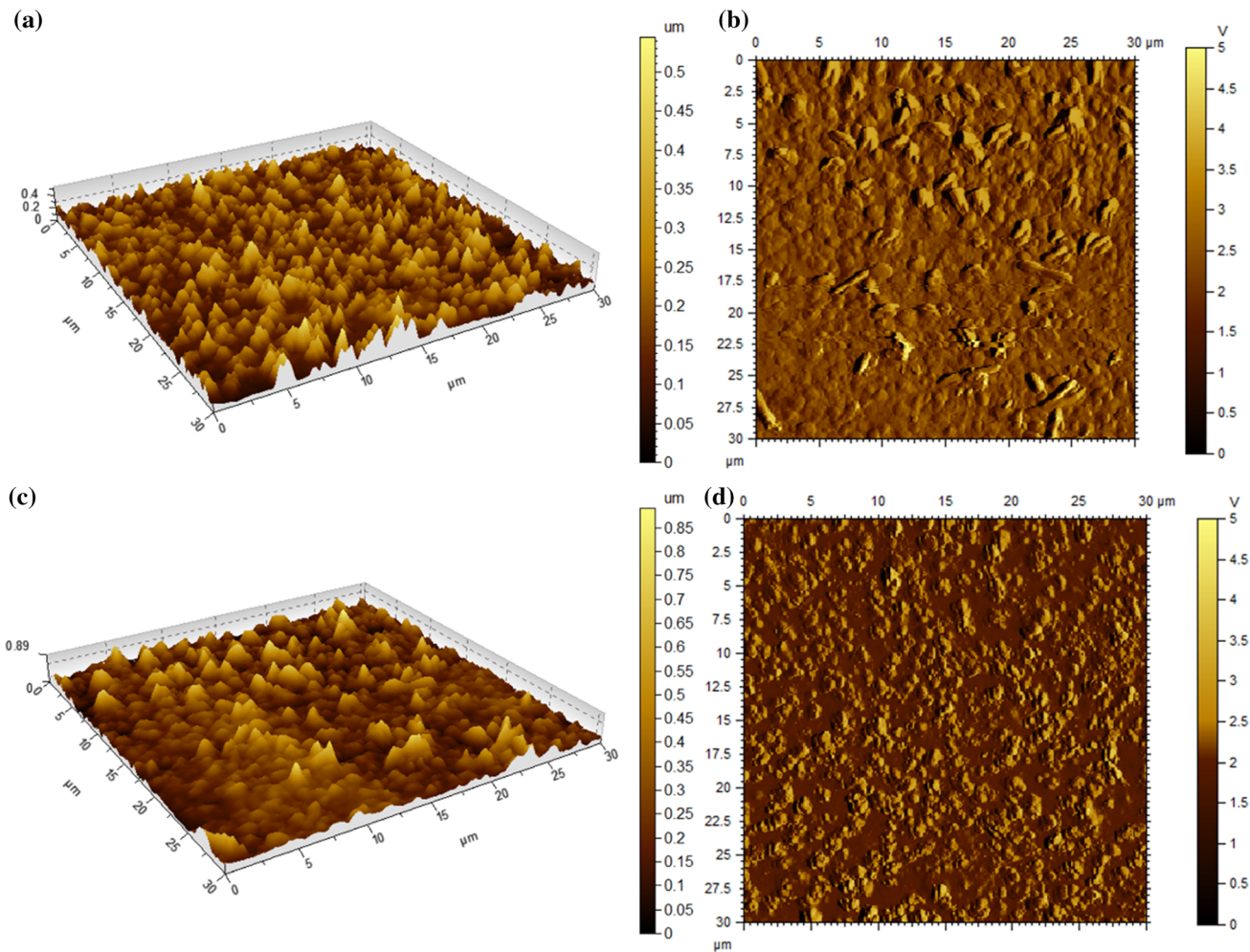


Figure 9 AFM images of NR vulcanizates: **a** 3D view of untreated NR, **b** amplitude of untreated NR, **c** 3D view of sorbitol-treated NR, and **d** amplitude of sorbitol treated NR composites.

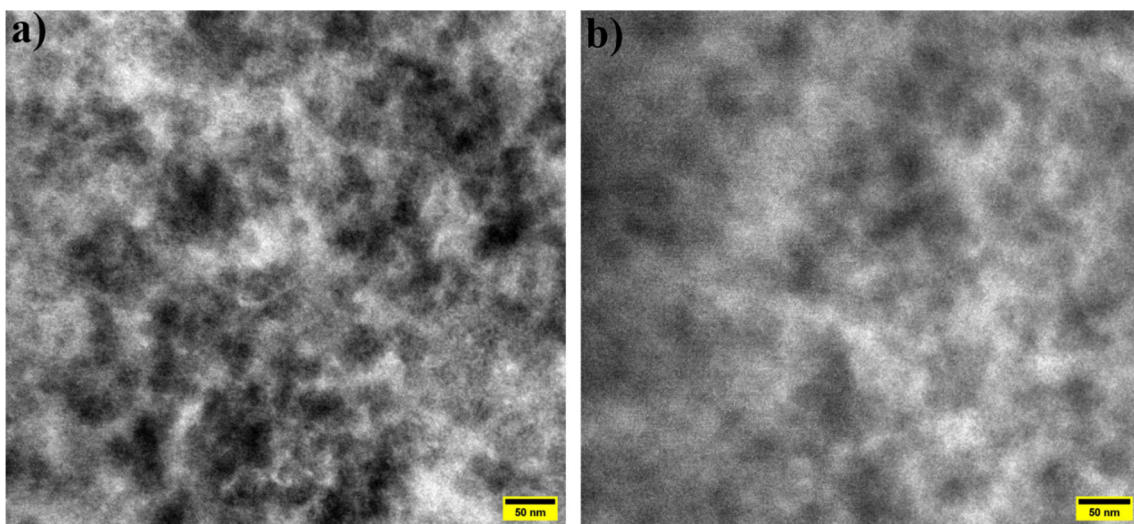


Figure 10 Transmission electron microscope (TEM) micrographs of filled **a** untreated and **b** treated NR vulcanizates.

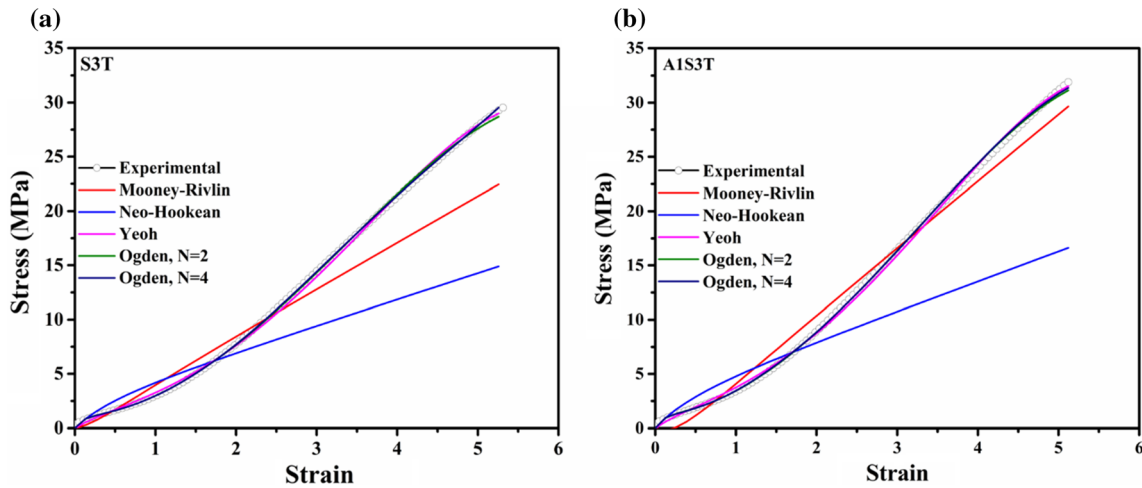


Fig. 11 Constitutive modelling of **a** control and **b** sorbitol-treated rubber composites.

Table 3 Correlation factor values for different material models

Material model	R^2 value	
	S3T	A1S3T
Mooney–Rivlin	0.852	0.891
Neo-Hookean	0.746	0.765
Yeoh	0.976	0.984
Ogden, $N = 2$	0.996	0.998
Ogden, $N = 4$	0.999	0.999

show that the Ogden material model with four variables ($N = 4$) fits the experimental data with maximum value of R^2 , which is further used to analyse other composites as well.

The shear modulus (G) of rubber composite can be calculated using Eq. 7, using which Young’s modulus can be calculated easily, which is three times the shear modulus.

$$G = \sum_{i=1}^4 \mu_i \tag{7}$$

The cross-link density of a rubber composite can be calculated using the Flory–Rehner equation and dynamic mechanical analysis (DMA), but nowadays, the calculation using material constants is being adapted [47]. The cross-link density (η) can be calculated using Ogden material model constants as

$$\eta = \frac{\sum_{i=1}^4 \mu_i}{R.T} \tag{8}$$

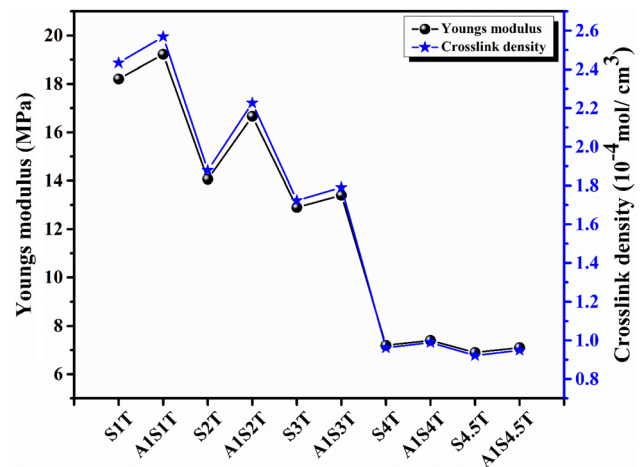


Fig. 12 Young’s modulus and cross-link density of treated and untreated NR vulcanizates.

where R is the universal gas constant and T is the absolute temperature.

The variation of Young’s modulus and cross-link density (from Ogden model) for rubber composites is shown in Fig. 12.

It can be distinctly observed that the cross-link density and Young’s modulus values are comparable between the sorbitol-treated and untreated NR vulcanizates till 30 phr loading of silica. Consequently, a minimal difference is detected for higher phr silica loading compounds, which is obviously due to the formation of network structure amidst the highly polar silica particles. Thus, the prediction of cross-link density from the Young’s modulus is thereby proved for the NR vulcanizates, as both of them

follow a similar trend as depicted in Fig. 12. Additionally, the correlation between the delta torque of MDR and cross-link density is also confirmed from their respective plots as explained in Sect. “Cure characteristics”.

Conclusions

The embodiment of sorbitol during the mastication stage originates bond with the functional groups of non-rubber substances of natural rubber. Therefore, the amine groups in natural rubber proteins cannot participate in curing reactions. The optimum cure time and scorch time of treated natural rubber compounds are slightly enhanced than the untreated ones. A significant improvement in the mechanical properties, i.e. tensile strength, elongation at break, tear strength, modulus, reinforcement index, abrasion resistance index, and rebound resilience of silica–carbon black-filled sorbitol-treated natural rubber vulcanizates, is reported. The heat build-up of the compounds eventually decreases along with the increment of silica loading. The introduction of a blocking agent surprisingly associates with the diminishing of the heat build-up more besides the dynamic compression set. Furthermore, a lower Payne effect is reported even at higher silica loading, which is a manifestation of the efficacy of sorbitol behind higher rubber–filler interaction. Consequently, based on all these mechanical and dynamic properties A1S3T compound was chosen as the superlative tyre tread compound and taken forward for dynamic mechanical analysis (DMA) study and morphology analysis. The lower $\tan \delta$ at 70 °C and homogeneous silica dispersion with minimal agglomeration conspicuously prove the superiority of sorbitol in high-silica-loaded natural rubber tyre tread compound. Finally the findings were validated using Ogden material model constants ($N = 4$) having correlation factor $R^2 = 0.999$.

Acknowledgements

The authors would like to acknowledge the Indian Institute of Technology Kharagpur and Apollo Tyres Pvt. Ltd, Chennai, for their financial support and all kinds of facilities. The authors are also thankful to the Central Research Facility of IIT Kharagpur for

carrying out the different characterization of the samples. The author also likes to thank Mr. Rajesh De, Junior Technician/Junior Laboratory Assistant, Rubber Technology Centre, IIT Kharagpur.

Author contribution

Abhijit Bera was involved in conceptualization, writing the original draft, and writing—reviewing and editing; Mohit Goswami and Debabrata Ganguly were responsible for writing—reviewing and editing, and methodology; Jyoti Prakash Rath, S. Ramakrishnan, and Job Kuriakose contributed to project administration; S. K. P. Amarnath took part in writing—reviewing and editing; and Santanu Chattopadhyay participated in supervision.

Funding

The authors acknowledge the Ministry of Education, India, Indian Institute of Technology Kharagpur, India, and Apollo Tyres Ltd. Chennai, India (Grant Number: IIT/SRIC/RT/TRF/2018–19/288), for funding and financial support during the course of this work.

Data and code availability

Available on special request.

Declarations

Conflict of interest The authors declare that there are no conflicts of interest to declare.

Supplementary Information: The online version contains supplementary material available at <https://doi.org/10.1007/s10853-022-08092-w>.

References

- [1] Bokobza L (2004) The reinforcement of elastomeric networks by fillers. *Macromol Mater Eng.* <https://doi.org/10.1002/mame.200400034>
- [2] Rattanasom N, Saowapark T, Deeprasertkul C (2007) Reinforcement of natural rubber with silica/carbon black hybrid filler. *Polym Test* 26:369–377. <https://doi.org/10.1016/J.POLYMERTESTING.2006.12.003>

- [3] Hassan HH, Ateia E, Darwish NA et al (2012) Effect of filler concentration on the physico-mechanical properties of super abrasion furnace black and silica loaded styrene butadiene rubber. *Mater Des.* <https://doi.org/10.1016/j.matdes.2011.05.005>
- [4] Noriman NZ, Ismail H (2012) Properties of styrene butadiene rubber (SBR)/recycled acrylonitrile butadiene rubber (NBRr) blends: The effects of carbon black/silica (CB/Sil) hybrid filler and silane coupling agent, Si₆₉. *J Appl Polym Sci* 124:19–27. <https://doi.org/10.1002/app.34961>
- [5] ten Brinke JW, Debnath SC, Reuvekamp LAEM, Noordermeer JWM (2003) Mechanistic aspects of the role of coupling agents in silica-rubber composites. *Compos Sci Technol* 63:1165–1174. [https://doi.org/10.1016/S0266-3538\(03\)00077-0](https://doi.org/10.1016/S0266-3538(03)00077-0)
- [6] Murakami K, Ilo S, Ikeda Y et al (2003) Effect of silane-coupling agent on natural rubber filled with silica generated in situ. *J Mater Sci.* <https://doi.org/10.1023/A:1022908211748>
- [7] Luginsland HD, Niedermeien W (2003) New reinforcing materials for rising tire performance demands. *Rubber World* 228:34–45
- [8] Kaewsakul W, Sahakaro K, Dierkes WK, Noordermeer JWM (2013) Optimization of rubber formulation for silica-reinforced natural rubber compounds. *Rubber Chem Technol* 86:313–329. <https://doi.org/10.5254/rct.13.87970>
- [9] Khanra S, Kumar A, Ghorai SK et al (2020) Influence of partial substitution of carbon black with silica on mechanical, thermal, and aging properties of super specialty elastomer based composites. *Polym Compos* 41:4379–4396. <https://doi.org/10.1002/PC.25720>
- [10] Rodgers B, Waddell W (2005) The science of rubber compounding. *Science and technology of rubber.* Wiley, Hoboken
- [11] Goswami M, Sharma S, Ghosh MM et al (2022) Finite element method based damage model to characterize effect of geometric configuration on fracture properties of elastomeric composites. *Mech Adv Mater Struct.* <https://doi.org/10.1080/15376494.2022.2051102>
- [12] Ganguly D, Bera A, Hore R et al (2022) Coining the attributes of nano to micro dual hybrid silica-ceramic waste filler based green HNBR composites for triple percolation: Mechanical properties, thermal, and electrical conductivity. *Chem Eng J Adv* 11:100338. <https://doi.org/10.1016/j.cej.2022.100338>
- [13] Khanra S, Ganguly D, Ghorai SK et al (2020) The synergistic effect of fluorosilicone and silica towards the compatibilization of silicone rubber and fluoroelastomer based high performance blend. *J Polym Res* 27:1–17. <https://doi.org/10.1007/S10965-020-02062-Z/FIGURES/15>
- [14] Sattayanurak S, Noordermeer JWM, Sahakaro K et al (2019) Silica-reinforced natural rubber: synergistic effects by addition of small amounts of secondary fillers to silica-reinforced natural rubber tire tread compounds. *Adv Mater Sci Eng* 2019:1–8. <https://doi.org/10.1155/2019/5891051>
- [15] Wang MJ (1999) The role of filler networking in dynamic properties of filled rubber. *Rubber Chem Technol.* <https://doi.org/10.5254/1.3538812>
- [16] Mihara S, Datta RN, Noordermeer JWM (2011) Flocculation in silica reinforced rubber compounds. *Rubber Chem Technol* 82:524–540. <https://doi.org/10.5254/1.3548262>
- [17] Dierkes WK, Noordermeer JWM (2004) Improving silica processing. *Rubber World* 229:8
- [18] Kaewsakul W, Sahakaro K, Dierkes WK, Noordermeer JWM (2015) Mechanistic aspects of silane coupling agents with different functionalities on reinforcement of silica-filled natural rubber compounds. *Polym Eng Sci.* <https://doi.org/10.1002/pen>
- [19] Goerl U, Hunsche A (1997) Investigations into the silica/silane reaction system. *Rubber Chem Technol* 70:608–623. <https://doi.org/10.5254/1.3538447>
- [20] Kaewsakul W, Sahakaro K (2012) Optimization of mixing conditions for silica-reinforced natural rubber tire tread compounds. *Rubber Chem Technol* 85:277–294. <https://doi.org/10.5254/rct.12.88935>
- [21] Ganguly D, Khanra S, Goswami D et al (2020) Controlling the mechanoadaptive properties of hydrogenated nitrile rubber by the incorporation of cementitious based industrial waste for downhole application. *Polym Compos* 41:4397–4410. <https://doi.org/10.1002/PC.25721>
- [22] Choi S, Nah C, Jo B (2003) Properties of natural rubber composites reinforced with silica or carbon black. *Influ Cure Accel Content Filler Dispers* 1389:1382–1389. <https://doi.org/10.1002/pi.1232>
- [23] Liengprayoon S, Dubreucq E, Sriroth K et al (2007) Lipid composition of Hevea brasiliensis latex and dry rubber: characterization and relation with some physical properties. *CRRI, India*
- [24] Kawahara S, Kakubo T, Sakdapipanich JT et al (2000) Characterization of fatty acids linked to natural rubber—role of linked fatty acids on crystallization of the rubber. *Polymer (Guildf)* 41:7483–7488. [https://doi.org/10.1016/S0032-3861\(00\)00098-7](https://doi.org/10.1016/S0032-3861(00)00098-7)
- [25] Nun-anan P, Wisunthorn S, Pichaiyut S et al (2020) Influence of nonrubber components on properties of unvulcanized natural rubber. *Polym Adv Technol* 31:44–59. <https://doi.org/10.1002/PAT.4746>
- [26] Kawahara S, Chaikumpollert O, Akabori K, Yamamoto Y (2011) Morphology and properties of natural rubber with

- nanomatrix of non-rubber components. *Polym Adv Technol* 22:2665–2667. <https://doi.org/10.1002/PAT.1803>
- [27] Zhou Y, Kosugi K, Yamamoto Y, Kawahara S (2017) Effect of non-rubber components on the mechanical properties of natural rubber. *Polym Adv Technol* 28:159–165. <https://doi.org/10.1002/PAT.3870>
- [28] Sarkawi SS, Dierkes WK, Noordermeer JWM (2013) The influence of non-rubber constituents on performance of silica reinforced natural rubber compounds. *Eur Polym J* 49:3199–3209. <https://doi.org/10.1016/J.EURPOLYMJ.2013.06.022>
- [29] Nimpai boon A, Sriring M, Kumarn S, Sakdapipanich J (2020) Reducing and stabilizing the viscosity of natural rubber by using sugars. *Interference Maillard React Between Protein Sugar*. <https://doi.org/10.1002/app.49389>
- [30] Lang F (2013) Cell volume control. *Seldin Geibisch's Kidney* 1:121–141. <https://doi.org/10.1016/B978-0-12-381462-3.00005-7>
- [31] Bera A, Ganguly D, Ghorai SK et al (2022) Treatment of natural rubber with bio-based components: a green endeavor to diminish the silica agglomeration for tyre tread application. *Chem Eng J Adv*. <https://doi.org/10.1016/J.CEJA.2022.100349>
- [32] Sattayanurak S, Sahakaro K, Kaewsakul W et al (2020) Synergistic effect by high specific surface area carbon black as secondary filler in silica reinforced natural rubber tire tread compounds. *Polym Test* 81:106173. <https://doi.org/10.1016/J.POLYMERTESTING.2019.106173>
- [33] Prasertsri S, Rattanasom N (2011) Mechanical and damping properties of silica/natural rubber composites prepared from latex system. *Polym Test* 30:515–526. <https://doi.org/10.1016/j.polymertesting.2011.04.001>
- [34] Choi SS (2002) Improvement of properties of silica-filled natural rubber compounds using polychloroprene. *J Appl Polym Sci* 83:2609–2616. <https://doi.org/10.1002/APP.10201>
- [35] Rattanasom N, Prasertsri S, Ruangritnumchai T (2009) Comparison of the mechanical properties at similar hardness level of natural rubber filled with various reinforcing-fillers. *Polym Test* 28:8–12. <https://doi.org/10.1016/j.polymertesting.2008.08.004>
- [36] Prasertsri S, Rattanasom N (2012) Fumed and precipitated silica reinforced natural rubber composites prepared from latex system: Mechanical and dynamic properties. *Polym Test* 31:593–605. <https://doi.org/10.1016/J.POLYMERTESTING.2012.03.003>
- [37] Diez J, Bellas R, Ramírez C, Rodríguez A (2010) Effect of organoclay reinforcement on the curing characteristics and technological properties of SBR sulphur vulcanizates. *J Appl Polym Sci* 118:566–573. <https://doi.org/10.1002/APP.32431>
- [38] Ogbebor OJ, Farid AS, Okwu UN (2004) Properties of silica/clay filled heavy-duty truck tire thread formulation. *J Appl Polym Sci* 94:1024–1028. <https://doi.org/10.1002/APP.20921>
- [39] Diani J, Fayolle B, Gilormini P (2009) A review on the mullins effect. *Eur Polym J* 45:601–612. <https://doi.org/10.1016/J.EURPOLYMJ.2008.11.017>
- [40] Houwink R (1956) Slipping of molecules during the deformation of reinforced rubber. *Rubber Chem Technol* 29:888–893. <https://doi.org/10.5254/1.3542602>
- [41] Mullins L (1948) Effect of stretching on the properties of rubber. *Rubber Chem Technol* 21:281–300. <https://doi.org/10.5254/1.3546914>
- [42] Kraus G, Childers CW, Rollmann KW (1966) Stress softening in carbon black-reinforced vulcanizates. Strain rate and temperature effects. *J Appl Polym Sci* 10:229–244. <https://doi.org/10.1002/APP.1966.070100205>
- [43] Hamed GR, Hatfield S (1989) On the role of bound rubber in carbon-black reinforcement. *Rubber Chem Technol* 62:143–156. <https://doi.org/10.5254/1.3536231>
- [44] Fu W, Wang L, Huang J et al (2019) Mechanical properties and mullins effect in natural rubber reinforced by grafted carbon black. *Adv Polym Technol*. <https://doi.org/10.1155/2019/4523696>
- [45] Goswami M, Ghosh MM, Dalmiya MS et al (2020) A finite element method based comparative fracture assessment of carbon black and silica filled elastomers: reinforcing efficacy of carbonaceous fillers in flexible composites. *Polym Test* 91:106856. <https://doi.org/10.1016/J.POLYMERTESTING.2020.106856>
- [46] Goswami M, Mandloi BS, Kumar A et al (2020) Optimization of graphene in carbon black-filled nitrile butadiene rubber: constitutive modeling and verification using finite element analysis. *Polym Compos* 41:1853–1866. <https://doi.org/10.1002/PC.25503>
- [47] Goswami M, Ghorai SK, Sharma S et al (2021) Nonlinear fracture assessment and nanomechanical deformation of elastomeric composites: development of finite element model and experimental validation. *Polym Compos* 42:3572–3592. <https://doi.org/10.1002/pc.26080>

Publisher's Note Springer Nature remains neutral with regard to jurisdictional claims in published maps and institutional affiliations.

Springer Nature or its licensor (e.g. a society or other partner) holds exclusive rights to this article under a publishing agreement with the author(s) or other rightsholder(s); author self-archiving of the accepted manuscript version of this article is solely governed by the terms of such publishing agreement and applicable law.